Modulus and adhesion of Sylgard 184, Solaris, and Ecoflex 00-30 silicone elastomers with varied mixing ratios

Daniel R. Darby, Zhuoyun Cai, Christopher R. Mason, and Jonathan T. Pham[*]

Department of Chemical and Materials Engineering, University of Kentucky, Lexington, KY 40506, USA

E-mail: Jonathan.Pham@uky.edu

Abstract: Two-part, commercial silicone elastomers are used in a variety of fundamental soft materials research and industrial applications due to their wide availability, ease of use, low cost, and mechanical tunability. This work seeks to create a library of moduli for three common elastomer systems with varied mixing ratios: Sylgard 184, Solaris, and Ecoflex 00-30, as well as provide a comparison of their adhesive properties. Shear storage moduli are quantified using parallel plate oscillatory shear rheology. The work of debonding is measured with spherical probe adhesion testing, and the static, advancing, and receding contact angles are measured via goniometer. Sylgard 184 can have shear moduli ranging from ~0.5 kPa-620 kPa, Solaris from ~0.6 kPa-175 kPa, and EF from ~1.3 kPa-35 kPa measured at a frequency of 0.01 rad/s. In general, increasing mixing ratios creates softer samples. Additionally, softer samples are universally more adhesive, regardless of the material system. When comparing the different material systems, Sylgard 184 is generally the most adhesive, followed closely by Solaris, and then by Ecoflex 00-30. Our study offers a baseline dataset of modulus values and comparative adhesion to help researchers determine an appropriate commercial silicone for their application.

1. Introduction

Silicone elastomers have wide reaching usage in both academia and industry.[1,2] Their tunable properties and easy moldability make them ideal candidates for stretchable and wearable electronics,[3,4] microfluidics,[4,5] biomaterials,[6–8] cosmetics,[1,9] and soft robotics.[1,4,10–15] Additionally, the ability to tune their mechanical and interfacial properties, combined with their commercial availability in simple, two-part systems, make silicones useful for fundamental studies on soft materials, including but not limited to adhesion,[9,16–20] friction,[21–23] wetting,[24,25] cavitation,[26] wrinkling,[17,27–29] fracture,[22,26,30] and cell-surface viability.[8,14,31–33] These elastomers mostly comprise polydimethylsiloxane (PDMS) and, in some cases, additional fillers such as nanoparticles.[1,34,35] Commonly, commercial systems use a platinum catalyst to activate a vinyl-hydride reaction for curing, referred to as hydrosylation.[9,36–38] Additionally, these elastomer systems can be enhanced through the addition of non-covalent bonds to enhance toughness and dissipate energy.[39–41] Although many silicones are available on the market, a few of the most widely implemented are Sylgard 184,[4,5,32,42,43] Solaris,[30,44] and Ecoflex 00-30.[4,16,45] Their widespread use has led to studies on their mechanical properties as a function of variables like strain rate, processing conditions, manufacturer, and mixing ratio of the two parts.[1,4,5,32,34,38,46,47] By manipulating the two-part mixing ratios away from factory recommendations, the moduli of the materials can be tuned. For example, Wang et al demonstrated that decreasing the amount of crosslinking agent decreases the resulting modulus for Sylgard 184, and proposed an empirical relation to predict the modulus as a function of mixing ratio.[48] Their empirical relationship works well for moduli above ~500 kPa; however, even softer materials, which are of particular interest for adhesive and biomaterials applications, were not considered. Yu, et al. investigated the PDMS-PDMS adhesion of Sylgard 184 and Ecoflex 00-30.[16] In their study, PDMS hemispherical probes were indented into PDMS surfaces and the Johnson-Kendall-Roberts (JKR) method was used to calculate a work of separation. While this study yields insight into adhesion of PDMS systems, it only varies mixing ratios of Sylgard 184 and investigates exclusively PDMS-PDMS adhesion.

Although Sylgard 184 has been a staple for fundamental studies, other silicone kits have become popular over recent years that offer slightly different properties while maintaining the two-part, one-pot synthetic simplicity. For example, Solaris is a two-part system that contains fewer fillers that was developed as a coating for photovoltaic cells.[44] Ecoflex 00-30 is widely used to mimic skin for special effects applications in movies and costumes, and is popular in the soft composites and robotics community for its high stretchability and toughness.[4,11,16,45,49,50] However, Ecoflex 00-30 is not optically clear, while Sylgard 184 and Solaris are transparent. Despite the increasing use of both materials, the effect of mixing ratio on their mechanical and interfacial properties is not well characterized within a single study. This limits the ability to compare these silicone elastomers or develop new experimental protocols using commercial silicones.

This contribution seeks to provide a baseline dataset of low-frequency shear moduli of Sylgard 184, Solaris, and Ecoflex 00-30 with mixing ratios varied from their factory recommendations (**Figure 1**a). Additionally, we compare their works of debonding to glass using a spherical probe adhesion test (Figure 1b,c). Our results show that Sylgard 184 is generally more adhesive and has a large available modulus range, while Ecoflex 00-30 and Solaris have smaller moduli ranges and are less adhesive. Using our moduli data table, contact angles are compared for the different elastomers with similar moduli, which are consistent with our adhesion results. We expect that our data will aid researchers in determining which of these systems and what mixing ratio best fit their end-use. Although many pathways are available for creating silicones with tunable properties, these two-part kits offer a simple, easily accessible route to tune material properties for several fields of research and engineering.

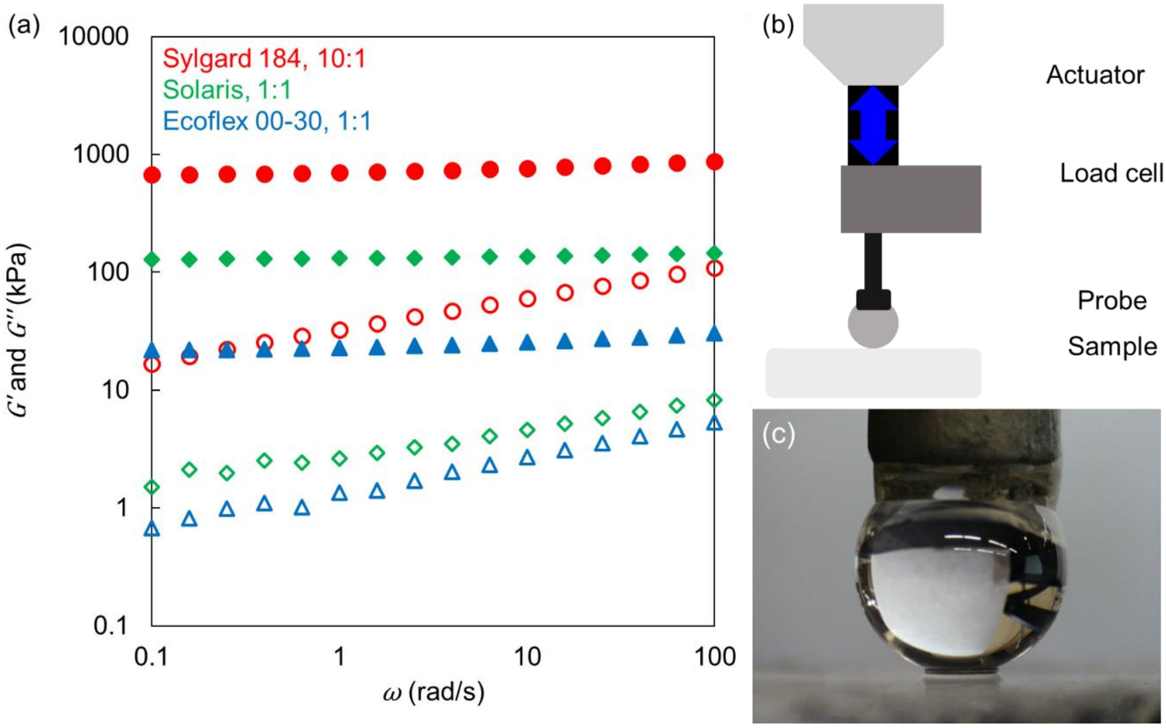

Figure 1: (a) Overlaid rheological data showing G' (filled symbols) and G'' (unfilled symbols) for Sylgard 184 (red, circles), Solaris (green, diamonds), and Ecoflex 00-30 (blue, triangles) at factory recommended mixing ratios. (b) A schematic of the probe adhesion testing apparatus used for adhesion measurements and (c) a side-view image from an adhesion test using a 6.35 mm diameter spherical glass probe on Sylgard 184.

2. Materials and Methods

2.1 Materials

All materials were used as obtained with no additives. Dow Sylgard 184 (SY) was purchased from Ellsworth Adhesives, Solaris (SO) and Ecoflex 00-30 (EF) from Smooth-On Inc., and polyacrylic acid (PAA, $M_n = 1800$ g/mol) from Sigma Aldrich. 5 cm round plastic petri dishes and deionized water (Ward's Science) were purchased from VWR.

2.2 Sample preparation

We prepared ~5 g samples in 5 cm diameter round petri dishes at selected mixing ratios by weight. First, petri dishes were UV/Ozone treated for 5 minutes to increase wettability. Then each dish was treated with 1 mL of 0.5 wt% PAA/H_2O solution that was spread across the bottom of the dish, and excess solution was removed with a pipette. Dishes were then dried in an oven at ~65°C. The PAA allows a hydrophilic barrier to form between the silicones and their dishes to mitigate sticking that occurred on some samples, with the aid of a small amount of water. To create the silicone samples, appropriate weights of each component of a sample were mixed vigorously for ~2 minutes in a 20 mL vial, and then poured in the petri dishes. The liquid silicone mixtures in the petri dishes were then placed under vacuum until all bubbles were removed. The dishes were placed into an oven for 60-65 hours at ~65°C for curing.

2.3 Parallel plate shear rheology

A TA Discovery HR-2 rheometer equipped with 25 mm aluminum plates was used to characterize the low-frequency moduli of our samples. To remove the samples from their petri dishes, we first used a 25 mm diameter punch from Grainger Equipment to cut the samples. Then a small amount of water was applied under the edge of the sample, which is drawn beneath the silicone by the PAA layer to allow for clean removal. Every sample underwent an amplitude sweep at 10 rad/s from 0.0125% to 1.25% strain to confirm that the strain existed in the linear regime. Frequency sweeps were all conducted at 0.1% strain (as confirmed by the amplitude sweep to be within the linear regime) from 0.01 rad/s—100 rad/s (Figure S1). The shear storage modulus is taken at 0.01 rad/s and assumed to be reasonably close to time-independent as the modulus change with frequency approaches a plateau.

2.4 Adhesion testing

A custom-built spherical probe adhesion tester (Figure 1b) is used to measure force and displacement,[51] while the contact is being imaged with a side-view camera to measure the contact area, A_0 (Figure 1c). 6.35 mm diameter optical sapphire doped glass spheres (Edmund Optics) were attached to screws that were then fed into a load cell (GSO-10, Transducer Techniques). The load cell is attached to a high precision linear actuator (L-239.50SD, Physik

Instrumente) to control displacement. The linear actuator was controlled with LabVIEW, and force vs. distance data was recorded during all steps. Samples were prepared using the method described above. Samples are indented at a rate of 0.1 mm/s to a depth of ~0.2 mm and allowed to dwell for 30 s. The probe was then retracted at a rate of 0.1 mm/s until complete detachment. Force data was then divided by the contact area to yield an apparent stress during pull-off, $\sigma = F/A_0$. This allowed for each adhesion test to provide a work of debonding (W_{db}). W_{db} was found by taking the integral of the stress vs displacement curve produced from each adhesion test.

2.5 Contact angle measurements

A goniometer (ramé-hart, 100-00) is used to measure the macroscopic static water contact angles on the elastomers. 4 μL deionized water drops are placed on the elastomer by using a microsyringe assembly (ramé-hart). Pictures of drops are captured using a digital camera and analyzed with ImageJ and using Dropsnake to extract macroscale contact angle data. For advancing and receding contact angles, a goniometer with an automatic dispensing system is used. The dispensing system injects and withdraws water on the sample surface with a constant inject/withdraw speed (0.1 μL/s). The advancing angles are taken as the measured contact angle when the contact line depins and expands during water injection, while the receding angles are obtained when the water contact line depins and start moving backwards during water withdrawal. The recorded videos are analyzed with ImageJ and using the Contact Angle plugin to extract macroscale contact angle data.

2.6 Uncrosslinked molecule extraction

After mechanical or adhesive characterization, three samples each of 10:1 and 35:1 Sylgard 184, 1:1 and 5:1 Solaris, and 1:1 Ecoflex 00-30 were prepared for uncrosslinked molecule extraction. Circular samples ~25 mm in diameter and ~4 mm thick were cut in half.

One half of each sample was set aside for comparison, while the other half was placed in a tared vial, and the mass of the sample recorded (M_i). Tared vials were then filled with hexane and allowed to swell for ~72 hours. Solvent was refreshed after ~24 and ~48 hours. Solvent was removed via pouring. Samples were dried for ~24 hours at ~65°C. Samples continued drying until a constant weight was obtained (M_f). % extractable, uncrosslinked material was calculated as $(M_i - M_f)/M_i$. Three samples of each mixing ratio were taken and the calculated % uncrosslinked chains were averaged.

3. Results and discussion

SY has with a factory recommended mixing ratio of 10:1 Base to crosslinking agent (CA). Both SO and EF come with a 1:1 part B to part A recommendation from the manufacturer. In our experiments, SY samples are tested at mixing ratios from 5:1 to 70:1, SO samples are tested from 0.5:1 to 20:1, and EF samples are tested from 0.5:1 to 60:1. Outside of these ranges, the materials became challenging to manipulate. SY samples range in low-frequency shear storage modulus (G') from ~0.5 kPa-620 kPa (**Figure 2**a**)**, SO samples ranged from ~0.6 kPa-175 kPa (Figure 2b), and EF samples ranged from ~1.3 kPa-35 kPa (Figure 2c). To obtain these modulus values, we tested multiple samples several times across multiple weight ratios to account for experimental batch-to-batch variance. We also made samples from different batches of each product to account for manufacturer batch-to-batch variance. For SY, the moduli generally decrease with increasing Base:CA ratio from the 10:1 recommendation. The modulus drops precipitously at first, in an evidently exponential fashion. While the factory recommended mixing ratio (10:1) produces a G' of ~620 kPa, double the ratio (20:1) yields ~190 kPa and increasing to triple the ratio (30:1) yields ~59 kPa. For the Solaris system, the moduli display a similar trend: the moduli decrease when increasing the mixing ratios (B:A). While the factory recommended mixing ratio yields a material with G'~120 kPa, 5x the recommended ratio (5:1) yields ~31 kPa and 10x (10:1) yields ~8.5 kPa. For the EF kit, the factory recommended mixing ratio (1:1) gives a shear modulus of ~27 kPa, which is consistent with the manufacturer datasheet. A 5:1 mixing ratio yields ~17 kPa while higher ratios can lead to moduli on the order of a kPa (e.g. 60:1 gives ~1.3 kPa). In general, both SY and SO show a continuous curve that appears exponential, while EF does not. Although EF does not follow an exponential pattern, the trend of decreasing moduli with increasing mixing ratios remains consistent.

For a more direct comparison between systems, we introduce a "Factor from Factory Recommendation" parameter, FFR, which considers mixing ratios in relation to factory recommendations. The FFR is obtained simply by dividing the mixing ratios by the factory recommendation and plotted with G' for each system (Figure 2d). SO and EF have a higher relative modulus change when considering the FFR. This may also explain the increased noise in SO and EF data at high mixing ratios, where crosslinking stoichiometries become further from their recommendations. Across all systems, it is evident that increasing mixing ratios decreases G'. This is a result of decreased crosslinking per volume in the networks.[32,48] Additionally, decreasing crosslinking by changing the mixing ratio of commercial silicone kits leaves a greater number of free chains in the networks. Free chains are uncrosslinked polymer chains that remain inside the polymer network after curing due to unbalanced stoichiometry.[32] These free chains can also decrease moduli by expanding the polymer network.[32,52,53] For example, at the factory recommended ratios, the amount of extractable material is ≈4.5%, 12% and 55% by weight for the Sylgard 184 (10:1), Solaris (1:1), and Ecoflex (1:1), respectively. The presence of these free chains, in addition to polymer backbone molecular weight differences and potential fillers, likely play a synergistic role in the mechanical properties at both factory recommended mixing ratios and other mixing ratios.

In addition to increasing the mixing ratio, we also halved the mixing ratio below factory recommendations to 5:1 for SY, and down to 1:2 for SO and EF. While 1:2 SO and

EF show increased modulus, likely due to increased crosslinking, SY 5:1 decreases in modulus. This decrease in SY suggests that excess crosslinker from the unbalanced stoichiometry can also lower modulus. We also point out that SY shows the least batch to batch variance of the three systems.

To provide quantitative values for the moduli for the three systems, **Table 1** reports the low-frequency G' values for different mixing ratios. Low-frequency moduli are used to compare the systems in a case where they are approaching equilibrium and the storage modulus is near a plateau (Figure S1). Note that although we plot every data point in Figure 2, the table includes averaged values within certain mixing ratios for clarity and brevity. In general, these data shows that SY has a wider modulus range, followed by SO and then EF. It should also be noted that we are reporting shear modulus values as directly measured. However, it is often convenient to know the Young's modulus. Assuming a Poisson's ratio of $\nu = 0.5$, which is common for elastomers, the Young's modulus can be calculated as $E = 3G$.

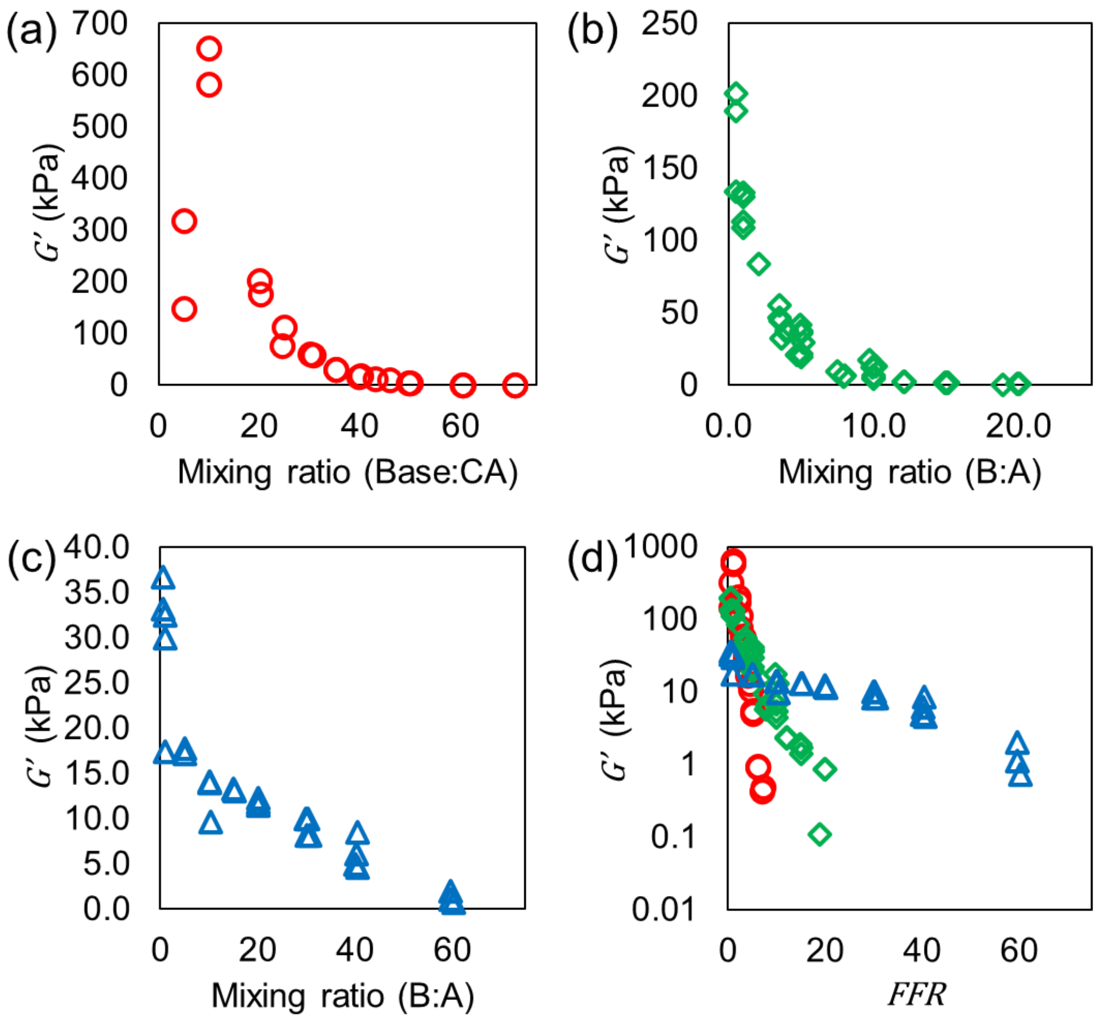

Figure 2: Plots of low-frequency (0.01 rad/s) shear storage moduli, G', for (a) Sylgard 184 (red, circles), (b) Solaris (green, diamonds), and (c) Ecoflex 00-30 (blue, triangles) as a function of Base to crosslinking agent (Base:CA) ratio for Sylgard 184 or part B to part A (B:A) ratio for Solaris and Ecoflex 00-30. (d) Plot of G' vs the factor from factory recommended mixing ratio (FFR) for each measured modulus.

Table 1: Low-frequency (0.01 rad/s) moduli of commercially available, two-part silicone elastomers with varied mixing ratios.

SY		SO		EF	
Mixing Ratio (Base:CA)	G' (kPa),	Mixing Ratio (B:A)	G' (kPa)	Mixing Ratio (B:A)	G' (kPa)
5	234 ± 120	0.5	175 ± 36	0.5	35 ± 2.4
10	620 ± 49	1.0	120 ± 12	1	27 ± 8.1
20	190 ± 19	3.5	49 ± 5.5	5	17 ± 0.4
30	59 ± 1.5	5.0	31 ± 8.9	10	13 ± 2.2
40	18 ± 0.8	10.0	8.5 ± 4.1	20	12 ± 0.4
50	5.4 ± 0.4	12.1	2.3 ± 0.03	30	9.1 ± 1.0
60	0.9 ± 0.1	15.0	1.7 ± 0.2	40	6.0 ± 1.8
71	0.5 ± 0.05	19.6	0.6 ± 0.4	60	1.3 ± 0.6

To investigate the adhesive properties of these commercial silicones as a function of mixing ratios, we use a glass spherical probe adhesion test to measure the work of debonding (W_{db}). W_{db} is obtained by integrating the stress vs. displacement measured during pull-off to quantify the energy dissipated during breaking of the silicone-glass interface. It should be noted that this is not the work of adhesion in the thermodynamic sense, calculated from surface energies, but an empirically measured macroscale value gathered from probe adhesion tests run at a constant rate of 0.1 mm/s, an indentation depth of 0.2 mm, and a 30 s contact time (or dwell time). The selected depth, δ, ensures that sample thickness is large enough that effects from the rigid underlying substrate does not impact the adhesive measurement.[54,55] The dwell time is selected to allow for relaxation of the softest materials tested (Figure S2). To confirm that the mechanical properties of each sample are in the expected range prior to adhesion testing, moduli are measured at a frequency of 0.1 rad/s. This frequency was selected to increase the testing throughput by reducing the time required for frequency sweeps, and because it corresponds to the adhesion testing velocity via the relation $\omega R/4\pi = v_{eff}$, where v_{eff} is an effective linear velocity (Equation S1). However, it should be noted that the higher frequency test will yield slightly higher G' values, but consistent with the trends in Figure 2. W_{db} is plotted against G' for the three material systems in **Figure 3**. In general, W_{db} increase as G' decreases for all samples. Softer materials usually display higher adhesion as a result of increased contact and deformability,[56,57] but this trend is likely exacerbated by an increase in free chains that may also lead to capillary behaviors.[24,33,52,58,59] When comparing the different material systems, EF is generally less adhesive at similar modulus values to SY and SO. For example, if we consider the W_{db} at a modulus of ~10 kPa, SY has the highest W_{db} at ~3.0 J/m^2 with SO at ~2.7 J/m^2, and EF has the lowest adhesion at ~1.0 J/m^2. Considering a higher modulus of ~100 kPa, SY maintains a higher adhesion on average at ~0.7 J/m^2 while SO gives a W_{db} at ~0.1 J/m^2 (EF cannot achieve this high of a modulus). At lower moduli, we find more scatter in the data for the EF and SO systems. This can be attributed to the increased mixing ratio required to achieve a low modulus, which has significant departure from the designed stoichiometry of the factory recommendation. For example, 45:1 SY is 4.5x the factory recommendation while 10:1 SO is 10x the factory recommendation, which have similar moduli at $G' \sim 10$ kPa (Figure 2d, Table 1). This higher deviation from designed mixing ratio may introduce more heterogeneity into the polymer networks of SO and EF relative to SY. In general, these commercial systems may include adhesion promoters or other fillers, like silica in Sylgard 184.[34,35] However, there are significant changes in the amount of free extractable chains as we modify the mixing ratios from the factory recommendation. For example, at a low frequency modulus of ~30 kPa, the amount of extractable material is ≈24%, 26%, and 55% for the Sylgard 184 (35:1), Solaris (5:1), and Ecoflex (1:1), respectively. The difference in adhesion between Sylgard 184 and Solaris samples of the same modulus (~30 kPa), which also have similar % of extractable material, suggests that the fillers present in Sylgard 184 may act as adhesion promoters. Moreover, it is interesting to note that there is a significant difference in color before and after extraction for the Ecoflex, going from cloudy to opaque white, while little change is seen in Solaris or Sylgard 184 (Figure S3). This illustrates that different fillers can be a large component.

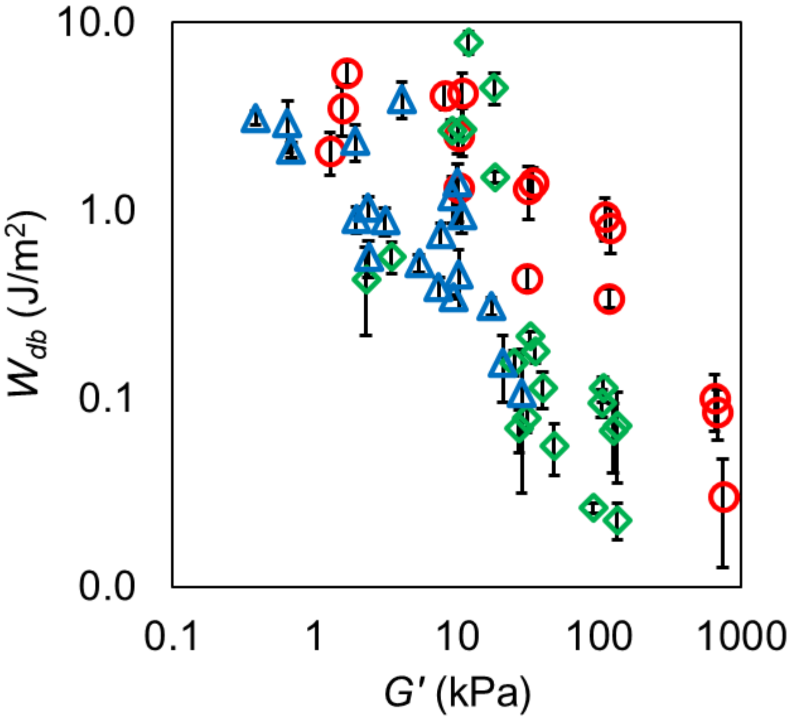

Figure 3: Plot of W_{db} vs G' for the three tested systems. Red circles represent Sylgard 184, green diamonds represent Solaris, and blue triangles represent Ecoflex 00-30. Each data point is an average of 5 adhesion tests. Error bars denote one standard deviation. Moduli are measured with 25 mm parallel plate shear rheology at 0.1% strain and 0.1 rad/s frequency.

As an additional support of adhesion results, we also measure the static (θ_S), advancing (θ_A) and receding (θ_R) contact angles with water. To compare SY, SO and EF elastomers without modulus variance, we control the modulus to $G' \approx$10 kPa for all three systems (Figure S1). The samples are sufficiently thick (>1 mm) to exclude a potential effect of thickness on wetting properties.[60–62] EF has the smallest static contact angle at θ_S = 110.7°± 3.4°, while SO and SY have relatively similar contact angles of θ_S = 120.1°± 1.5° and 121.5°± 1.4°, respectively (**Figure 4**). Based on static contact angles, SY and SO are more hydrophobic than EF. On the other hand, contact angle hysteresis ($CAH = \theta_A - \theta_R$) can provide more insight into drop-surface adhesion. Generally, higher CAH indicates higher adhesion.[63,64] SO and EF have similar CAH at 44.8°± 3.0° and 47.2°± 4.5°, respectively, while SY has the largest CAH at 83.5°± 2.1° (Figure 4). The CAH results indicate that EF and SO are less adhesive (or more slippery) than SY, even though θ_S for SO is similar to SY. The EF and SY results are consistent with our adhesion measurements that show EF is the least adhesive and SY is the most adhesive at $G' \approx 10$ kPa. The difference in the wetting properties of these three different commercial PDMS elastomers may be due to differences in surface tension, fillers, or the amount of free chains in the elastomers[24,65,66].

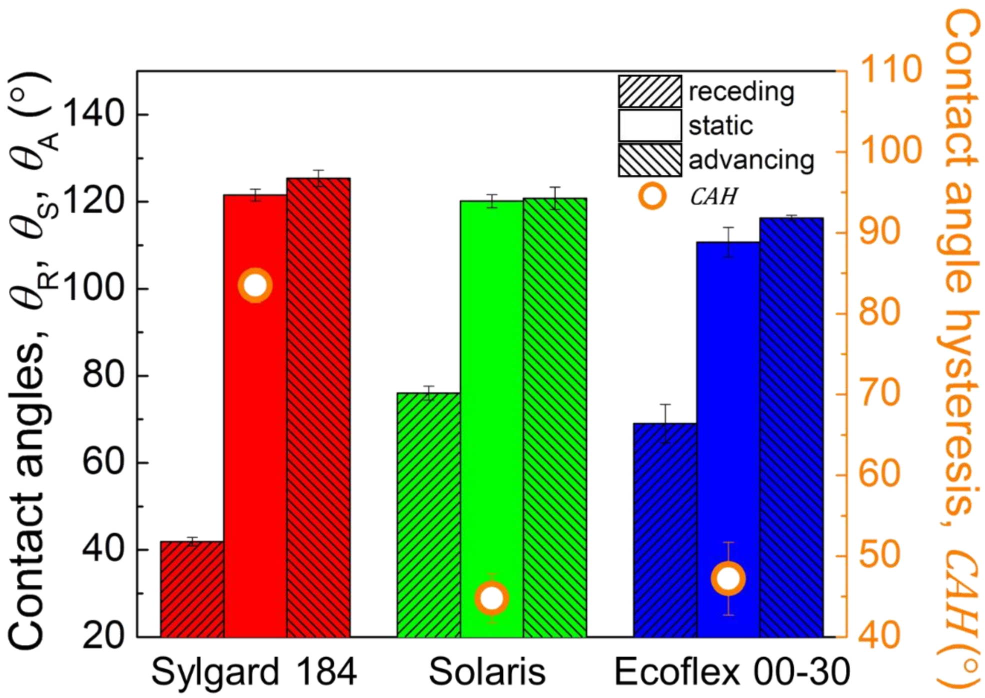

Figure 4. Water contact angles on Sylgard 184 (red), Solaris (green), and Ecoflex 00-30 (blue) elastomers at $G' \approx 10$ kPa. Receding (forward slash patterned bars), advancing (backslash slash patterned bars) and static (solid bars) contact angles differ among Sylgard 184, Solaris, and Ecoflex 00-30. The corresponding contact angle hysteresis is shown as orange open circles.

4. Conclusion

We have quantified how changing mixing ratios of two-part, commercial, silicone elastomers affect their low-frequency shear storage moduli. In general, increasing the Base to curing agent, Base:CA, or part B to part A, B:A, mixing ratios of the tested two-part elastomers decreases the modulus. This is a result of decreasing the crosslinking density and likely introducing uncrosslinked polymer chains to the elastomer network. Within the tested mixing ratios, Sylgard 184 can produce elastomers with a modulus range from ~0.5 kPa to ~620 kPa, Solaris from ~0.6 kPa to ~175 kPa, and EF from ~1.3 kPa to ~35 kPa. Using spherical probe adhesion tests, we demonstrate that Ecoflex 00-30 is generally the least adhesive of the materials while Sylgard 184 is generally the most adhesive; we further confirm this trend with contact angle experiments. Our study offers a baseline set of data on mechanical and interfacial properties of two-part silicone kits, which aims to help researchers select appropriate materials for their end-use applications.

Acknowledgements

The authors thank Winnie Huang for helpful discussions. This work was primarily supported by the National Science Foundation (NSF) KY-EPSCoR, OIA-1849213, and partially by NSF CBET-2043732.

Received: ((will be filled in by the editorial staff))
Revised: ((will be filled in by the editorial staff))
Published online: ((will be filled in by the editorial staff))

References

1. Mazurek, P.; Vudayagiri, S.; Skov, A. L. *Chem. Soc. Rev.* **2019**, *48*, 1448.
2. Sharfeddin, A.; Volinsky, A. A.; Mohan, G.; Gallant, N. D. *J. Appl. Polym. Sci.* **2015**, *132*, 42680.
3. Wu, Q.; Xiong, H.; Peng, Y.; Yang, Y.; Kang, J.; Huang, G.; Ren, X.; Wu, J. *ACS Appl. Mater. Interfaces* **2019**, *11*, 19534.
4. Park, S.; Mondal, K.; Treadway, R. M.; Kumar, V.; Ma, S.; Holbery, J. D.; Dickey, M. D. *ACS Appl. Mater. Interfaces* **2018**, *10*, 11261.
5. Johnston, I. D.; McCluskey, D. K.; Tan, C. K. L.; Tracey, M. C. *J. Micromechanics Microengineering* **2014**, *24*, 035017.
6. Chen, H.; Brook, M. A.; Sheardown, H. *Biomaterials* **2004**, *25*, 2273.
7. Brook, M. A. *Biomaterials* **2006**, *27*, 3274.
8. Pham, J. T.; Xue, L.; Del Campo, A.; Salierno, M. *Acta Biomater.* **2016**, *38*, 106.
9. Moon, J.; Huh, Y.; Park, J.; Kim, H. W.; Choe, Y.; Huh, J.; Bang, J. *ACS Appl. Polym. Mater.* **2020**, *2*, 2444.
10. Glick, P.; Suresh, S. A.; Ruffatto, D.; Cutkosky, M.; Tolley, M. T.; Parness, A. *IEEE Robot. Autom. Lett.* **2018**, *3*, 903.
11. Markvicka, E. J.; Bartlett, M. D.; Huang, X.; Majidi, C. *Nat. Mater.* **2018**, *17*, 618.
12. Zhu, L.; Wang, Y.; Mei, D.; Ding, W.; Jiang, C.; Lu, Y. *ACS Appl. Mater. Interfaces* **2020**, *12*, 31725.
13. Perju, E.; Shova, S.; Opris, D. M. *ACS Appl. Mater. Interfaces* **2020**, *12*, 23432.
14. Gökaltun, A.; Kang, Y. B. A.; Yarmush, M. L.; Usta, O. B.; Asatekin, A. *Sci. Rep.* **2019**, *9*, 7377.
15. Vatankhah-Varnosfaderani, M.; Daniel, W. F. M.; Everhart, M. H.; Pandya, A. A.; Liang, H.; Matyjaszewski, K.; Dobrynin, A. V.; Sheiko, S. S. *Nature* **2017**, *549*, 497.
16. Yu, Y.; Sanchez, D.; Lu, N. *J. Mater. Res.* **2015**, *30*, 2702.
17. Davis, C. S.; Martina, D.; Creton, C.; Lindner, A.; Crosby, A. J. *Langmuir* **2012**, *28*, 14899.
18. Son, H.; Chau, A. L.; Davis, C. S. *Soft Matter* **2019**, *15*, 6375.
19. Twohig, T.; Croll, A. B. *Soft Matter* **2021**, *17*, 9170.
20. Nase, J.; Ramos, O.; Creton, C.; Lindner, A. *Eur. Phys. J. E* **2013**, *36*, 1.
21. Langowski, J. K. A.; Dodou, D.; Kamperman, M.; Van Leeuwen, J. L. *Front. Zool.* **2018**, *15*, 32.
22. Zhang, B.; Shiang, C. S.; Yang, S. J.; Hutchens, S. B. *Exp. Mech.* **2019**, *59*, 517.
23. Viswanathan, K.; Sundaram, N. K. *Wear* **2017**, *376–377*, 1271.
24. Cai, Z.; Skabeev, A.; Morozova, S.; Pham, J. T. *Commun. Mater.* **2021**, *2*, 21.
25. Jensen, K. E.; Sarfati, R.; Style, R. W.; Boltyanskiy, R.; Chakrabarti, A.; Chaudhury, M. K.; Dufresne, E. R. *Proc. Natl. Acad. Sci. U. S. A.* **2015**, *112*, 14490.
26. Poulain, X.; Lefèvre, V.; Lopez-Pamies, O.; Ravi-Chandar, K. *Int. J. Fract.* **2017**, *205*, 1.
27. Chen, D.; Yoon, J.; Chandra, D.; Crosby, A. J.; Hayward, R. C. *J. Polym. Sci. Part B Polym. Phys.* **2014**, *52*, 1441.
28. Milner, M. P.; Jin, L.; Hutchens, S. B. *Soft Matter* **2017**, *13*, 6894.
29. Rencheck, M. L.; Rodriguez, R.; Miller, N. A.; Davis, C. S. *J. Polym. Sci. Part B Polym. Phys.* **2019**, *57*, 15.
30. Zhang, B.; Hutchens, S. B. *Soft Matter* **2021**, *17*, 6728.
31. Fischer, R. S.; Myers, K. A.; Gardel, M. L.; Waterman, C. M. *Nat. Protoc.* **2012**, *7*, 2056.
32. Glover, J. D.; McLaughlin, C. E.; McFarland, M. K.; Pham, J. T. *J. Polym. Sci.* **2020**, *58*, 343.

33. Glover, J. D.; Pham, J. T. *Soft Matter* **2020**, *16*, 5812.
34. Ortiz-Acosta, D.; Densmore, C. *LA-UR-12-25325: Sylgard Cure Inhibition Characterization*; **2012**.
35. Brounstein, Z.; Zhao, J.; Geller, D.; Gupta, N.; Labouriau, A. *Polymers* **2021**, *13*, 3125.
36. Lukin, R. Y.; Kuchkaev, A. M.; Sukhov, A. V.; Bekmukhamedov, G. E.; Yakhvarov, D. G. *Polymers* **2020**, *12*, 1.
37. Guo, L. J. *Adv. Mater.* **2007**, *19*, 495.
38. Cai, L. H.; Kodger, T. E.; Guerra, R. E.; Pegoraro, A. F.; Rubinstein, M.; Weitz, D. A. *Adv. Mater.* **2015**, *27*, 5132.
39. Bui, R.; Brook, M. A. *Polymer* **2019**, *160*, 282.
40. Filippidi, E.; Cristiani, T. R.; Eisenbach, C. D.; Herbert Waite, J.; Israelachvili, J. N.; Kollbe Ahn, B.; Valentine, M. T. *Science.* **2017**, *358*, 502.
41. Shi, J.; Zhao, N.; Yan, D.; Song, J.; Fu, W.; Li, Z. *J. Mater. Chem. A* **2020**, *8*, 5943.
42. Palchesko, R. N.; Zhang, L.; Sun, Y.; Feinberg, A. W. *PLoS One* **2012**, *7*, 51499.
43. Saha, T.; Fang, J.; Mukherjee, S.; Dickey, M. D.; Velev, O. D. *ACS Appl. Mater. Interfaces* **2021**, *13*, 8071.
44. Kataruka, A.; Hutchens, S. B. *Soft Matter* **2019**, *15*, 9665.
45. Heo, S. H.; Kim, C.; Kim, T. S.; Park, H. S. *Adv. Funct. Mater.* **2020**, *30*, 2002360.
46. Kroll, R.; Tsori, Y.; Doss, B. L.; Rahmani Eliato, K.; Lin, K.; Ros, R. *Soft Matter* **2007**, *15*, 1776.
47. Case, J. C.; White, E. L.; Kramer, R. K. *Soft Robot.* **2015**, *2*, 80.
48. Wang, Z.; Volinsky, A. A.; Gallant, N. D. *J. Appl. Polym. Sci.* **2014**, *131*, 1.
49. Chen, J.; Zhu, Y.; Chang, X.; Pan, D.; Song, G.; Guo, Z.; Naik, N. *Adv. Funct. Mater.* **2021**, 2104686.
50. Bilodeau, R. A.; Mohammadi Nasab, A.; Shah, D. S.; Kramer-Bottiglio, R. *Soft Matter* **2020**, *16*, 5827.
51. Darby, D. R.; Lai, E.; Holten-Andersen, N.; Pham, J. T. *Adv. Mater. Interfaces* **2021**, 2100319.
52. Dorogin, L.; Persson, B. N. J. *Soft Matter* **2018**, *14*, 1142.
53. Krpovic, S.; Dam-Johansen, K.; Skov, A. L. *J. Appl. Polym. Sci.* **2021**, *138*, 50380.
54. Shull, K. R.; Ahn, D.; Chen, W.-L.; Flanigan, C. M.; Crosby, A. J. *Macromol. Chem. Phys* **1998**, *199*, 489.
55. Bartlett, M. D.; Crosby, A. J. *Langmuir* **2013**, *29*, 11022.
56. Johnson, K. L. *Tribol. Int.* **1998**, *31*, 413.
57. Shull, K. R. *Mater. Sci. Eng. R Reports* **2002**, *36*, 1.
58. Pham, J. T.; Schellenberger, F.; Kappl, M.; Butt, H. J. *Phys. Rev. Mater.* **2017**, *1*, 4.
59. Tiwari, A.; Dorogin, L.; Bennett, A. I.; Schulze, K. D.; Sawyer, W. G.; Tahir, M.; Heinrich, G.; Persson, B. N. J. *Soft Matter* **2017**, *13*, 3602.
60. Style, R. W.; Boltyanskiy, R.; Che, Y.; Wettlaufer, J. S.; Wilen, L. A.; Dufresne, E. R. *Phys. Rev. Lett.* **2013**, *110*, 066103.
61. Zhao, M.; Dervaux, J.; Narita, T.; Lequeux, F.; Limat, L.; Roché, M. *Proc. Natl. Acad. Sci. U. S. A.* **2018**, *115*, 1748.
62. Pu, G.; Severtson, S. J. *J. Phys. Chem. C* **2011**, *115*, 18729.
63. ElSherbini, A. I.; Jacobi, A. M. *Prog. Colloid Polym. Sci.* **2004**, *128*, 57.
64. ElSherbini, A. I.; Jacobi, A. M. *J. Colloid Interface Sci.* **2006**, *299*, 841.
65. Hourlier-Fargette, A.; Antkowiak, A.; Chateauminois, A.; Neukirch, S. *Soft Matter* **2017**, *13*, 3484.
66. Sedev, R. V.; Petrov, J. G.; Neumann, A. W. *J. Colloid Interface Sci.* **1996**, *180*, 36.

Table of contents entry.

The impact of mixing ratio on mechanical and interfacial properties of commercial, two-part silicone elastomer systems is investigated using shear rheology, spherical probe adhesion testing, and contact angle measurement (static, advancing and receding). Here it is shown that varying mixing ratios further from factory recommended settings yields softer, more adhesive elastomers.

Daniel R. Darby, Zhuoyun Cai, Christopher R. Mason, Jonathan T. Pham*

Modulus and adhesion of Sylgard 184, Solaris, and Ecoflex 00-30 silicone elastomers with varied mixing ratios